JOURNAL OF SOLID STATE CHEMISTRY 93, 228–235 (1991)

$Sr_2Bi_2O_5$: A Structure Containing Only 3-Coordinated Bismuth

C. C. TORARDI

Central Research and Development, Du Pont Central Research, Experimental Station, P.O. Box 80356, Wilmington, Delaware 19880-0356

J. B. PARISE

Mineral Physics Institute and Department of Earth and Space Sciences, State University of New York, Stony Brook, New York 11794-2100

AND A. SANTORO, C. J. RAWN, R. S. ROTH, AND B. P. BURTON

National Institute of Standards and Technology, Gaithersburg, Maryland 20899

Received December 11, 1990; revised March 19, 1991

The bismuth(III) strontium oxide $Sr_2Bi_2O_5$ has been synthesized in the low-temperature form, and studied using both single-crystal X-ray and powder neutron diffractometry. All bismuth atoms are in an unusual threefold coordination with oxygen. The compound crystallizes in the orthorhombic space group *Pnma* with $Z = 4$ and X-ray cell parameters $a = 14.261(3)$, $b = 6.160(2)$, $c = 7.642(3)$ Å. A superlattice, visible in long exposure precession photographs, exists along c (2×3.8 Å). This is due to the ordering of oxygen and vacancies along the c-axial direction, and to resulting displacements of the Bi atoms along c. The structure consists of an ordered intergrowth, along the a-axial direction, of slabs of inverse NiAs-type, with composition Sr_2O_4 and strings of Bi–O–Bi···□···Bi–O–Bi···, where □ represents an oxygen vacancy. © 1991 Academic Press, Inc.

1. Introduction

This paper represents part of a body of work undertaken in our laboratories to elucidate the phase diagrams and structures of phases in the systems M–Bi–O, where M = Ca and Sr (*1–4*). We report here the synthesis and structure of the low-temperature form of $Sr_2Bi_2O_5$. In a previous publication (*5*), we described the synthesis and structure of a compound, $Ca_4Bi_6O_{13}$, containing Bi in both 5- and 3-coordination with oxygen. In the latter compound, the existence of square-pyramidal BiO_5 units was not unusual, but the formation of pyramidal BiO_3 moieties, having Bi with low coordination, was surprising. This geometry for bismuth was also seen and described recently in the high-temperature superconductors $Bi_2Sr_{3-x}M_xCu_2O_{8+\delta}$ (M = Ca, Y) (*6*) and $Bi_{2-x}Pb_xSr_2CuO_{6+\delta}$ (*6, 7*). In $Ca_4Bi_6O_{13}$, the 3-coordinate Bi atoms form Bi–O–Bi···□···Bi–O–Bi··· chains. The alternation of oxygen and vacancies (□), along with short and long Bi–Bi distances, gives rise to a superlattice in the direction

0022-4596/91 $3.00

of the chains. $Sr_2Bi_2O_5$ is built of similar chains and contains bismuth exclusively in 3-coordination with oxygen.

2. Experimental

2.1. Synthesis and Characterization

The powder specimen for neutron diffraction characterization was synthesized by weighing and mixing a 40-g batch composed of $SrCO_3$ and Bi_2O_3 in the stoichiometric ratio of Sr/Bi atoms equal to 1 : 1. This mixture was heated several times at various temperatures to attain single-phase equilibria. The mixed powder was first isopressed into a pellet and heated to 700°C, ground, repressed, and heated to 850°C. Four more heat treatments, using only hydrostatic pressing, were made at 900°C, with grinding and repressing between each heat treatment. Each heating cycle was held at maximum temperature for about 16–24 hr. The X-ray powder diffraction pattern showed only the orthorhombic compound $Sr_2Bi_2O_5$ (*1*). This low-temperature form of $Sr_2Bi_2O_5$ transforms at 925 ± 5°C to the body-centered tetragonal structure (*1, 2*), a nonstoichiometric solid solution whose structure has recently been determined (*8*) (discussed below). Single crystals of the low-temperature form were obtained in two different ways. The first technique consisted of heating the precrystallized powder $Sr_2Bi_2O_5$ with a halide flux, $(Na_{0.5}K_{0.5})Cl$, and cooling at 3°C/hr from 900 to 640°C with charge/flux ratios from 98 : 2 to 50 : 50. These crystals were used for preliminary X-ray structural work. Larger crystals were obtained by cooling a melt of the appropriate composition in Au tubes, crushing the resultant "quenched" liquid, and annealing the crushed particles at 850°C for 258 hr. Crystals from this batch were used for the final X-ray structural refinement.

Crystals of $Sr_2Bi_2O_5$ are pale-yellow plates flattened along [100]. Optical examination under a microscope showed no evidence of twinning. The crystals were found by the precession method to be orthorhombic, with systematic absences indicating space groups $Pnma$ or $Pn2_1a$. Subsequent refinement confirmed the adequacy of the choice of the centric space group. The unit cell obtained from precession photographs and refined by least-squares analysis of an X-ray powder diffraction pattern (*1*) has parameters $a = 14.307(1)$, $b = 6.1713(4)$, $c = 7.6524(4)$ Å. This unit cell compares well with that of previous work (*9*), where $a = 14.293(2)$, $b = 6.172(1)$, and $c = 7.651(2)$ Å for their material. Precession photographs, single crystal diffractometer data, and neutron powder diffractograms are consistent with the presence of a strong subcell along c, such that $c_{subcell} = \frac{1}{2}c = 3.825$ Å.

2.2 Structure Determination

Single crystal X-ray diffraction data were collected on an Enraf–Nonius CAD diffractometer using the experimental conditions given in Table I. Cell parameters for the larger unit cell with $c = 2c_{subcell}$ were determined from 25 reflections with $6 < \theta < 23°$. All reflections were corrected for Lorentz and polarization effects, and an analytical absorption correction was applied (*10*). Structure solution was initiated using a Patterson-function peak-search/solution algorithm developed by J. C. Calabrese (*11*). A trial structure based on the positions of the Bi and Sr atoms was refined, and the oxygen atom positions were found using difference Fourier synthesis. At this stage, it was obvious that all atoms, save one oxygen position O(1), were approximately related by a translation along the c-axial direction of (0, 0, $\frac{1}{2}$). The observed doubling of the $c_{subcell}$ was presumed to be due in part to the ordering of one oxygen along this direction, and in part to displacements of the Bi atoms along the c direction to give alternating long and short Bi–Bi distances. The structure solution reduced the determination to which one

TABLE I

SUMMARY OF X-RAY DIFFRACTION DATA FOR $Sr_2Bi_2O_5$

Color	Pale yellow
Size (mm)	0.03 × 0.13 × 0.22
Crystal system	Orthorhombic
Space group	*Pnma* (No. 62)
a (Å)	14.261(3)
b (Å)	6.160(2)
c (Å)	7.642(3)
Temperature (°C)	20
Volume (Å^3)	671.3
Z	4
Formula weight	673.195
Calculated density (g/cc)	6.660
μ(Mo) (cm^{-1})	674.08
Diffractometer	Enraf–Nonius CAD4
Radiation (graphite monochromator)	Mo$K\alpha$
Data collected	4251
Max 2θ (deg)	60.0
Max h, k, l	20, 8, 10
Data octants	+++, −++, −+−, ++−
Scan method	ω
Absorption correction	Analytical
Transmission factors, range	0.009–0.138
No. of unique data ($I > 3.0\sigma(I)$)	522
Refinement method	Full-matrix least squares on F
Anomalous dispersion	Bi, Sr
Weighting scheme	$\propto [\sigma^2(I) + 0.0009I^2]^{-1/2}$
Atoms refined	Aniso: Bi, Sr, O(1) Iso: all other O
Parameters varied	40
Data/parameter ratio	13.05
R	0.027
R_w	0.027
Error of fit	1.04
Secondary extinction coeff. (mm)	$0.15(1) \times 10^{-4}$

TABLE II

SUMMARY OF NEUTRON POWDER DIFFRACTION AND REFINEMENT DATA FOR $Sr_2Bi_2O_5$

Monochromatic beam	Reflection 220 of a Cu monochromator
Wavelength	1.553(1) Å
Horizontal divergences	10, 20, and 10′ arc for the in-pile, monochromatic beam, and diffracted beam collimators, respectively
Sample container	Vanadium can of ~10 mm diameter
Cell parameters	a = 14.3019(3), b = 6.1718(1), c = 7.6524(1) Å
Space group	*Pnma*
R_{wp}	0.069
R_n	0.057
χ^2	2.43

of two possible relative positions of oxygen and vacancies exists for this material.

In order to elucidate the refined oxygen-vacancy ordering scheme, a neutron powder diffraction study was initiated. Data were collected at the BT1 station of the reactor at the National Institute of Standards and Technology with the experimental conditions given in Table II. All peaks could be indexed on the basis of the primitive unit cell found from the single crystal X-ray study (compare Tables I and II). Initial positional and thermal parameters for the profile refinement were those obtained from the single crystal X-ray data, and the scattering lengths used in the refinement were b(Bi) = 0.853, b(Sr) = 0.702, b(O) = 0.581 × 10^{-12} cm. Proceeding from this model, the atomic positional and isotropic thermal parameters (Table III), unit cell parameters, as well as the instrumental parameters, such as peak halfwidths, diffractometer zero, and background, were refined. The two possible ordering schemes for oxygen atom O(1) lead to quite different discrepancy indices; the nuclear R-factors derived from the powder neutron study, which could best be compared with the values obtained from the X-ray study, were 0.074 and 0.178 for O(1) sited at z = 0.37 and z = 0.87, respectively.

TABLE III

POSITIONAL[a] AND ISOTROPIC-THERMAL PARAMETERS[b] FOR $Sr_2Bi_2O_5$ FROM SINGLE CRYSTAL X-RAY AND POWDER NEUTRON DIFFRACTION DATA[c]

Atom	Site	x	y	z	B_{iso}(Å^2)
Bi(1)	4c	0.18467(5)	0.25	0.1188(6)	0.80(1)′
		0.1853(2)	0.25	0.1190(5)	0.8(1)
Bi(2)	4c	0.19104(6)	0.25	0.6336(5)	0.75(1)′
		0.1901(2)	0.25	0.6336(5)	0.8(1)
Sr(1)	4c	0.0668(1)	0.75	0.8676(12)	0.70(3)′
		0.0664(2)	0.75	0.8740(6)	0.7(1)
Sr(2)	4c	0.0553(1)	0.75	0.3707(13)	0.84(3)′
		0.0556(2)	0.75	0.3770(6)	0.8(1)
O(1)	4c	0.2420(8)	0.25	0.3712(20)	1.4(2)′
		0.2409(2)	0.25	0.3702(6)	1.8(1)
O(2)	8d	0.0871(5)	0.4892(12)	0.1344(12)	1.0(1)
		0.0875(2)	0.4877(4)	0.1273(6)	1.0(1)
O(3)	8d	0.0928(5)	0.0124(12)	0.6198(12)	1.1(1)
		0.0931(2)	0.0126(4)	0.6169(5)	1.0(1)

[a] Space group *Pnma*.

[b] Metal atoms and O(1) refined anisotropically using single-crystal X-ray data. B_{equiv} is given for these atoms.

[c] First line from X-ray data, second line from neutron data.

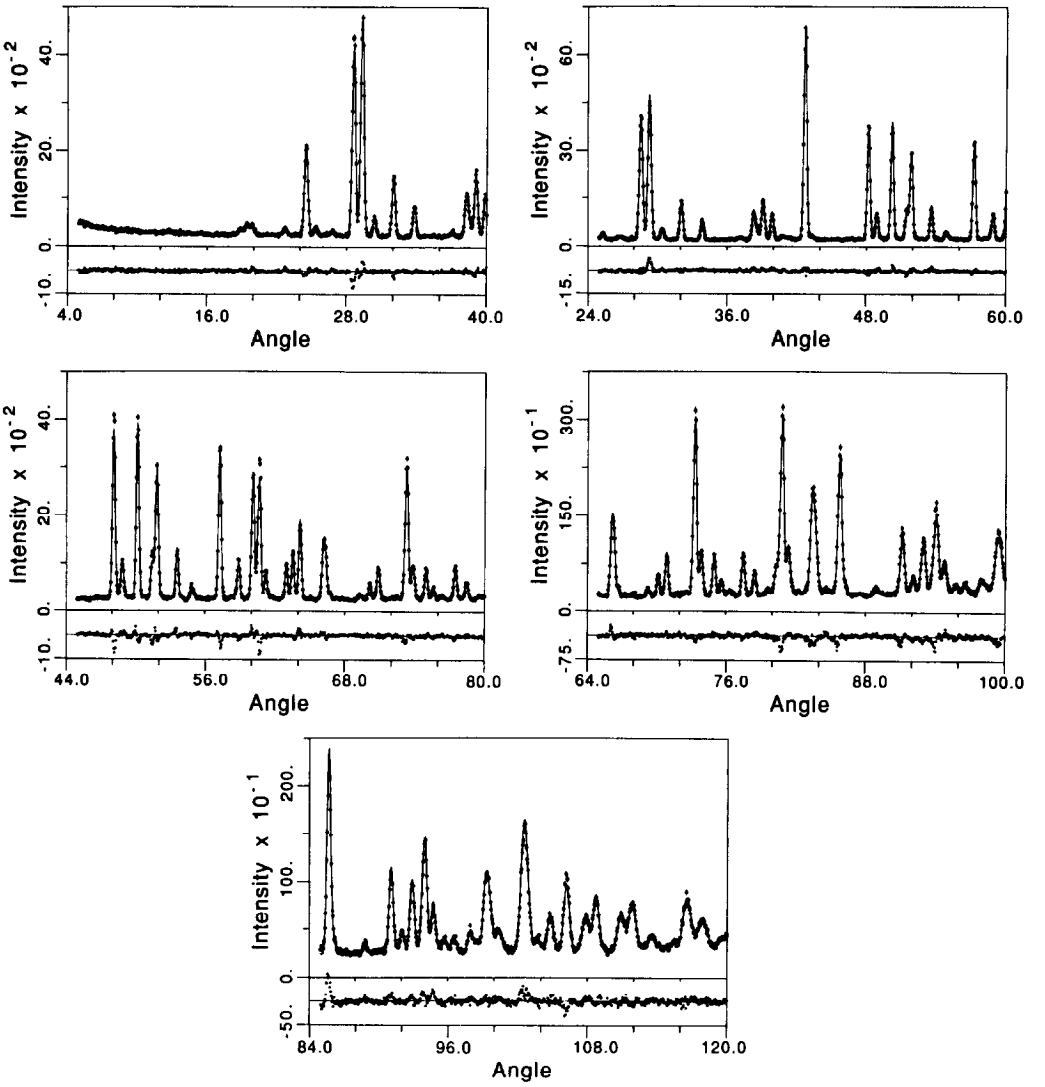

Fig. 1. Profile fit and difference plots for the neutron powder diffraction pattern of $Sr_2Bi_2O_5$.

Full refinements including the site occupancies for bismuth and strontium suggested they were fully occupied only by Bi and Sr, respectively. Figure 1 shows the profile fit and difference plots.

Armed with the neutron evidence for the position of atom O(1), the X-ray refinement proceeded apace. Only the model having O(1) with the positional coordinates given in Table III could be refined using the X-ray data. When O(1) was placed at the vacant position ($z + \frac{1}{2} = 0.8712$), the least-squares refinement shifted this atom along z, settling back into the originally occupied site ($z = 0.3712$). Further, O(1) had a relatively large isotropic thermal parameter (Table III) and was therefore refined anisotropically. The reason for this anisotropic motion is dis-

TABLE IV

ANISOTROPIC THERMAL PARAMETERS[a] (Å^2) FOR THE ATOMS OF $Sr_2Bi_2O_5$ FROM SINGLE-CRYSTAL X-RAY DIFFRACTION DATA

Atom	B_{11}	B_{22}	B_{33}	B_{12}	B_{13}	B_{23}
Bi(1)	1.02(2)	0.53(2)	0.85(4)	0.0(0)	0.09(5)	0.0(0)
Bi(2)	1.07(2)	0.55(2)	0.51(5)	0.0(0)	−0.13(4)	0.0(0)
Sr(1)	1.09(6)	0.51(6)	0.42(9)	0.0(0)	0.2(1)	0.0(0)
Sr(2)	1.24(5)	0.54(6)	0.64(7)	0.0(0)	−0.4(1)	0.0(0)
O(1)	1.2(4)	1.9(5)	1.1(4)	0.0(0)	0.3(5)	0.0(0)

[a] $\exp[-0.25(B_{11}h^2a^{*2} \ldots + 2(B_{12}hka^*b^* \ldots))]$.

cussed below. Full-matrix least-squares refinements including site occupancies, checked one at a time, confirmed the sites to be fully occupied. A final difference Fourier showed the strongest peak to be 2.76 e^- located 0.6 Å from Bi(1). Atomic positional and isotropic thermal parameters are given in Table III, and anisotropic thermal parameters for Bi, Sr and O(1) are shown in Table IV.

3. Results and Discussion

The structure of $Sr_2Bi_2O_5$ consists of the intergrowth of two simple structural elements. The first of these is the anti-nickel arsenide structure shown schematically in Fig. 2a. The structure of NiAs is usually envisioned as an hexagonally close-packed array of As atoms with Ni occupying all available octahedral interstitial sites. An alternative approach is to consider the coordination of the anion; in this case the As atom is surrounded by six cations in a trigonal-prismatic array (*12*). In the case of $Sr_2Bi_2O_5$, if the Bi and O(1) atoms are disregarded for the present, each Sr is surrounded by six nearest neighbors in a trigonal-prismatic arrangement. Indeed, as is shown in Fig. 2a, this segment of the structure can be derived from that of anti-NiAs by removal of two-thirds of the metal and one-third of the anion sites to give a slab with composition $Sr_2O_4^{4-}$. The structure is referred as being of the anti-NiAs-type since the cations, and not the anions, are in trigonal-prismatic coordination.

The second structural element is similar to the Bi_2O^{4+} chains first described for the compound, $Ca_4Bi_6O_{13}$ (*5*). These ···Bi–O–Bi···□···Bi–O–Bi··· chains (here □ represents a vacancy) are inserted between the anti-NiAs slabs and oriented in the *c*-axial direction as shown in Fig. 2b. The O(1) atom alternates with vacancies along the *c*-axial direction. As with $Ca_4Bi_6O_{13}$ (*5*), the lone pair of electrons associated with the Bi can be envisioned as being directed toward the vacant site as schematically represented in Fig. 3.

The two structural elements are stacked along the *a*-axial direction. They are connected via bonds between the Bi ions in the chains and O ions in the Sr–O slabs, and by a bond between Sr(1), in the anti-NiAs slab, and the O(1) atom in the chains, as shown in Figs. 2b and 4. As expected, the 7-coordi-

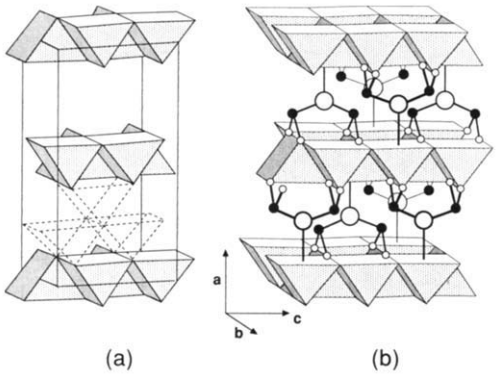

FIG. 2. (a) The unit cell of $Sr_2Bi_2O_5$ showing the SrO_6 trigonal prisms of composition Sr_2O_4; the corners represent the positions of oxygen atoms. Dotted lines depict the missing polyhedra which would complete the NiAs-type structure. The Sr_2O_4 composition is derived by the removal of two-thirds of the metal and one-third of the oxygen atoms from a 1 : 1 stoichiometry. (b) Position of $[Bi_2O]^{4+}$ groups of $Sr_2Bi_2O_5$ with respect to the slabs of $[Sr_2O_4]^{4+}$ shown in (a). Open and closed circles represent oxygen and bismuth sites, respectively. Only the oxygen atoms bonded to bismuth are shown as circles.

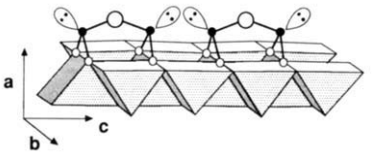

FIG. 3. A chain of 3-coordinated bismuth atoms in $Sr_2Bi_2O_5$ oriented along the *c* axis. The positions of the Bi 6*s* lone pair orbitals are represented in cartoon form.

nated Sr(1) atom has a slightly longer average bond length with oxygen, 2.610 Å, than does the 6-coordinated Sr(2) atom, 2.528 Å. In the *bc* plane, the rectangular face of the trigonal prism around Sr(1) is somewhat larger than that around Sr(2) because Sr(1) forms its additional bond to O(1) through this rectangular face, and is consequently displaced toward O(1).

Bismuth ions along the chain are not evenly spaced, thereby contributing to the "superstructure" observed along the *c*-axial direction. The distance between bismuth atoms bridged by O(1) is 3.935 Å, and the unbridged Bi–Bi separation is 3.710 Å. This is to be compared to the distances 3.865 and 3.341 Å found in the Bi–O chains of $Ca_4Bi_6O_{13}$ for the bridged and unbridged Bi–Bi distances, respectively. Because of the short unbridged distance in the latter compound, the lone-pair lone-pair repulsion would be substantial if the lone-pair orbitals were directed toward one another. However, a hybridization of the Bi 6*s* and 6*p* orbitals reduces the extent of the repulsion by tilting the lone-pair orbitals away from each other. This also displaces the bridging oxygen atom between the bismuth ions (*5*). Such an effect is minimal or nonexistent in $Sr_2Bi_2O_5$ because of the greater nonbridged Bi–Bi distance. The smaller difference in the short and long Bi–Bi separations relative to those in $Ca_4Bi_6O_{13}$ may be due to the presence of the larger strontium cations. Adjacent Bi–O chains in $Sr_2Bi_2O_5$ (Fig. 4) do not interact as evidenced by interchain Bi(1)–O(1) and Bi(2)–O(1) distances of 3.76 and 3.70 Å, respectively.

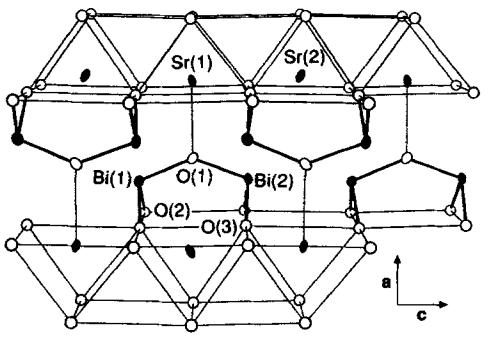

FIG. 4. An ORTEP (*16*) representation of the structure of $Sr_2Bi_2O_5$. The filled circles indicate the Bi and Sr sites. The anti-NiAs-type Sr–O slabs and the Bi–O chains (see text) are connected via Sr(1)–O(1) bonds.

The geometry around the bridging oxygen atom O(1), which also forms a bond to Sr(1), is trigonal planar because all four atoms (Bi(1), Bi(2), Sr(1), and O(1)) lie on a mirror plane. O(1) is constrained in its vibrational motion within the mirror plane because of its bonding. However, there are no bonds to O(1) out of the mirror plane. This allows O(1) to move more freely in the direction perpendicular to the mirror, the *b*-axial direction, and explains why the anisotropic B_{22} term is large (Table IV). The trigonal planar geometry, and the short average Bi(1)–O and Bi(2)–O bond lengths (2.05 and 2.06 Å, respectively), is suggestive of a π-bonding interaction between Bi and O(1). It should be noted, however, that the shortest Bi–O bonds are Bi(1)–O(2) and Bi(2)–O(3) (Table V). O(2) and O(3) are tetrahedrally coordinated, each forming bonds with one bismuth and three strontium atoms.

The structure of $Sr_2Bi_2O_5$ is distinct from that of the newly characterized phase $Ba_2Bi_2O_5$ (*13*). In the barium compound, bismuth is 4-coordinated in a pseudo-trigonal-bipyramidal geometry where one equatorial position is occupied by the lone pair of electrons. The four Bi–O bond lengths are 2.064, 2.075, 2.241, and 2.489 Å. However, if the

TABLE V

SELECTED INTERATOMIC DISTANCES (Å) AND ANGLES (DEG) CALCULATED FROM THE SINGLE-CRYSTAL X-RAY AND POWDER NEUTRON REFINEMENTS

Distance	X-ray	Neutron	Angle	X-ray	Neutron
Bi(1)—O(1)	2.095(15)	2.080(5)	O(1)—Bi(1)—O(2) ×2	102.3(4)	103.6(7)
—O(2) ×2	2.030(7)	2.028(6)	O(2)—Bi(1)—O(2)	93.1(4)	92.6(7)
Bi(2)—O(1)	2.133(14)	2.142(6)	O(1)—Bi(2)—O(3) ×2	100.8(4)	100.0(7)
—O(3) ×2	2.028(7)	2.022(9)	O(3)—Bi(2)—O(3)	92.4(4)	92.9(8)
Sr(1)—O(1)	2.727(11)	2.755(5)			
—O(2) ×2	2.612(11)	2.543(8)			
—O(2) ×2	2.643(7)	2.646(8)			
—O(3) ×2	2.517(11)	2.577(8)			
Sr(2)—O(2) ×2	2.459(11)	2.546(5)			
—O(3) ×2	2.554(11)	2.507(13)			
—O(3) ×2	2.571(7)	2.583(17)			

longest Bi–O bond (2.489 Å) is disregarded, then pairs of BiO_3 units bridged by one of the oxygen atoms may be described. The dimers do not form chains as do those in $Ca_4Bi_6O_{13}$ and $Sr_2Bi_2O_5$, and the Bi–$O_{bridging}$–Bi bond angle is not bent but linear (*13*).

4. Concluding Remarks

Most of the Sr–Bi–O and Ca–Sr–O phases reported to date are of the rhombohedral sillenite type (*14, 15*) in which the alkaline-earth metal and the bismuth are disordered and occupy the same crystallographic sites in high-symmetry crystal structures. The high-temperature form of $Sr_2Bi_2O_5$ has BiO_3 and SrO_6 units each with a disordered oxygen atom, and a site containing both bismuth and strontium (*8*). We have shown that the low-temperature phases, such as $Ca_4Bi_6O_{13}$ and $Sr_2Bi_2O_5$, have ordered cation arrangements and resulting lower symmetry. Research efforts in the characterization of low-temperature, ordered structures in the Ca–Bi, Sr–Bi, Sr–Bi–Cu, and Sr/Ca–Bi–Cu oxide systems have also uncovered a new low bismuth coordination environment. Thus far, bismuth in 3-coordination with oxygen exists only in systems containing the electropositive alkaline-earth cations Ca and Sr. It may be that these cations allow the Bi–O bonds to be more covalent in nature and therefore highly directional as observed. More examples of phases that incorporate this novel structural feature will be required in order to gain insight into these fascinating structure–bonding relationships.

Acknowledgment

The authors thank W. J. Marshall for the single-crystal selection and X-ray data collection.

References

1. R. S. ROTH, C. J. RAWN, B. P. BURTON, AND F. BEECH, *J. Res. NIST* **95,** 291 (1990).
2. N. M. HWANG, R. S. ROTH, AND C. J. RAWN, *J. Am. Ceram. Soc.* **73**[8], 2531 (1990).
3. B. P. BURTON, C. J. RAWN, R. S. ROTH, AND N. M. HWANG, *J. Res. NIST,* to be published (1991).
4. R. S. ROTH, N. M. HWANG, C. J. RAWN, B. P. BURTON, AND J. J. RITTER, *J. Am. Ceram. Soc.,* in press (1991).
5. J. B. PARISE, C. C. TORARDI, M.-H. WHANGBO, C. J. RAWN, R. S. ROTH, AND B. P. BURTON, *Chem. Mater.* **2,** 454 (1990).
6. C. C. TORARDI, J. B. PARISE, M. A. SUBRAMANIAN, J. GOPALAKRISHNAN, AND A. W. SLEIGHT, *Physica C* **157,** 115 (1989).

7. C. C. TORARDI, E. M. MCCARRON, P. L. GAI, J. B. PARISE, J. GHOROGHCHIAN, D. B. KANG, M.-H. WHANGBO, AND J. C. BARRY, *Physica C*, in press (1991).
8. C. C. TORARDI, R. S. ROTH, C. J. RAWN, J. B. PARISE, AND B. P. BURTON, in preparation.
9. R. GUILLERMO, P. CONFLANT, J. C. BOVIN, AND D. THOMAS, *Rev. Chim. Miner.* **15,** 153 (1978).
10. J. DE MEULENAER AND H. TOMPA, *Acta Crystallogr.* **19,** 1014 (1965).
11. All x-ray crystallographic calculations were performed on a Digital Equipment Corp. VAX 8800 computer using a system of programs developed by J. C. Calabrese.
12. A. F. WELLS, "Structural Inorganic Chemistry," 5th ed., p. 75, Oxford University Press (1984).
13. P. LIGHTFOOT, J. A. HRILJAC, S. PEI, Y. ZHENG, A. W. MITCHELL, D. R. RICHARDS, B. DABROWSKI, J. D. JORGENSEN, AND D. G. HINKS, *J. Solid State Chem.*, in press (1991).
14. L. G. SILLEN AND B. AURIVILLIUS, *Z. Kristallogr.* **101,** 483 (1939).
15. B. AURIVILLIUS, *Ark. Kemi Mineral. Geol.* **16A,** 1 (1943).
16. C. K. JOHNSON, "ORTEP: A Fortran Thermal-Ellipsoid Plot Program for Crystal Structure Illustration," Oak Ridge National Laboratory Report 5138 (1976).